LA-UR- 97-548

CONF-9606223--6

Title:

ANALYSIS AND SIMULATION OF A SMALL-ANGLE NEUTRON SCATTERING INSTRUMENT ON A 1 MW LONG PULSE SPALLATION SOURCE

Author(s): Glen A. Olah & Rex P. Hjelm

DISTRIBUTION OF THIS DOCUMENT IS UNLIMITED

RECEIVED
APR 10 1997
OSTI

Submitted to: "Journal of Neutron Research"

MASTER

Los Alamos
NATIONAL LABORATORY

Los Alamos National Laboratory, an affirmative action/equal opportunity employer, is operated by the University of California for the U.S. Department of Energy under contract W-7405-ENG-36. By acceptance of this article, the publisher recognizes that the U.S. Government retains a nonexclusive, royalty-free license to publish or reproduce the published form of this contribution, or to allow others to do so, for U.S. Government purposes. The Los Alamos National Laboratory requests that the publisher identify this article as work performed under the auspices of the U.S. Department of Energy.

Form No. 836 R5
ST 2629 10/91

DISCLAIMER

This report was prepared as an account of work sponsored by an agency of the United States Government. Neither the United States Government nor any agency thereof, nor any of their employees, make any warranty, express or implied, or assumes any legal liability or responsibility for the accuracy, completeness, or usefulness of any information, apparatus, product, or process disclosed, or represents that its use would not infringe privately owned rights. Reference herein to any specific commercial product, process, or service by trade name, trademark, manufacturer, or otherwise does not necessarily constitute or imply its endorsement, recommendation, or favoring by the United States Government or any agency thereof. The views and opinions of authors expressed herein do not necessarily state or reflect those of the United States Government or any agency thereof.

DISCLAIMER

Portions of this document may be illegible in electronic image products. Images are produced from the best available original document.

ANALYSIS AND SIMULATION OF A SMALL-ANGLE NEUTRON SCATTERING INSTRUMENT ON A 1 MW LONG PULSE SPALLATION SOURCE

Glenn A. Olah & Rex P. Hjelm

Manuel Lujan, Jr. Neutron Scattering Center
Los Alamos National Laboratory
Los Alamos, New Mexico, 87545
USA

Running Title:
Long-Pulsed SANS

Send correspondence to:

Rex P. Hjelm
H805
Los Alamos National Laboratory
Los Alamos, NM 87545 USA
Tel: 505-665-2372
FAX: 505-665-2676
e-mail: Hjelm@lanl.gov

ABSTRACT

We studied the design and performance of a small-angle neutron scattering (SANS) instrument for a proposed 1 MW, 60 Hz long pulsed spallation source at the Los Alamos Neutron Science Center (LANSCE). An analysis of the effects of source characteristics and chopper performance combined with instrument simulations using the LANSCE Monte Carlo instrument simulations package shows that the T_0 chopper should be no more than 5 m from the source with the frame overlap and frame definition choppers at 5.6 and greater than 7 m, respectively. The study showed that an optimal pulse structure has an exponential decaying tail with $\tau \approx 750$ μs. The Monte Carlo simulations were used to optimize the LPSS SANS, showing that an optimal length is 18 m. The simulations show that an instrument with variable length is best to match the needs of a given measurement. The performance of the optimized LPSS instrument was found to be comparable with present world standard instruments.

INTRODUCTION

Small-angle neutron scattering (SANS) is an important technique to consider on any neutron source, as there is high demand for this type of measurement in biology, polymer science, metallurgy, critical phenomena, etc. Science using SANS focuses on low resolution measurements probing large length scales of order 10 - 1000 Å. The inverse relation between length scale and momentum transfer, Q, which is related to the scattering angle 2θ and the incident neutron wavelength, λ, by

$$Q = \frac{4\pi}{\lambda}\sin\theta, \qquad 1$$

implies not only that the scattering intensity, I(Q), be measured at small angles, but the measurement also make use of long wavelengths. Thus, neutrons used for SANS measurements should be from a well equilibrated cold moderator source. Cold neutrons have significant equilibration times and therefore have relatively long pulse widths (~100 μs) even for decoupled moderators. On the other hand, coupled moderators have increased flux in this very low energy regime by making use of reflectors that feed neutrons back into the moderator, but at the expense of increasing the pulse width from between ~ 300 μs to greater than ~ 1 ms depending on the reflector/moderator characteristics [1]. The resulting long pulse structure gives low time of flight (TOF) resolution that is well matched to the geometry of the instrument, and has the great advantage of high intensity. These response times are not well matched to the ~ 1 μs pulse of a short pulsed spallation source (SPSS) , which is expensive to produce and which is limited on the total current to target, due to charge density limitation in the ring structures needed to produce a

short pulse. Thus, a long pulsed spallation source (LPSS) with a proton pulse width matched to the moderator response times is potentially beneficial for a SANS measurement.

A 1 MW LPSS will be available at the Los Alamos Neutron Science Center (LANSCE). This source uses a high intensity proton beam from the existing linac which will deliver proton pulses with 1 ms duration proton pulses at 60 Hz. Coupled liquid hydrogen moderators on this source will give a cold neutron flux that is approximately 0.25 that of CS-2 at the Institut Laue Langevin [1]. The purpose of this paper is to explore the design of a SANS instrument for the LANSCE 1MW LPSS and make comparisons of the performance of this instruments with SANS on an SPSS and continuous (reactor) sources. The LANSCE 1MW LPSS source parameters are not optimal for realizing the full potential gains from using time of flight (TOF) on an LPSS-SANS; nonetheless, we show that by making use of the good match between source characteristics, the instrument design and the needs of the measurement, an instrument can still be built that will be on par with D11 at the Institut-Laue Langevin. D11 provides one of the highest flux per resolution of any SANS instrument in the world.

DESIGN CONSIDERATIONS

Any new SANS instrument should be designed to meet the goals specified at the Berkeley LPSS workshop in 1995 [2]. Foremost among these goals is that new machines have significantly higher count rate in each resolution element. Thus, we consider the use of a high power LPSS using a coupled liquid hydrogen moderator. Improved signal-to-noise was deemed essential in using the additional count rate effectively. A need for variable resolution was seen to be important, extending from the traditional 10% $\sigma(Q)/Q$ to higher resolution values of 2%, as systems of greater complexity are considered. Finally good dynamic range, accessing a Q-domain of 0.001 - 0.5 $Å^{-1}$ was seen to be important in order to access as broad a domain of length scales as possible. We consider a design that meets these two later goals as closely as practical.

The basic design issues that need to be considered are the instrument geometry, the source characteristics and the number, positions and phasing of choppers. The basic rules or optimal instrument geometry have been understood for some time [3]. Thus, we use the cone rule to produce a beam that converges at the detector. The entrance and exit collimation apertures are as close to the source and the sample as possible, respectively, with the sample position half way between the source and the detector. The only issue here is the optimal instrument length, L, which is interrelated to choppers and source characteristics, and we consider the optimal length in some detail. We also look at the function of choppers, and analyze the rules governing performance on a SANS. The balance between the pulse length and the total integrated flux must be considered as well.

Choppers

There are three choppers with distinctly different functions that are needed in an LPSS, TOF SANS. The first is the T_0 chopper, which functions to prevent the initial flash of hot neutrons and γ radiation from reaching the detector. The second is the frame definition chopper, which serves to limit the band length so that TOF frames do not overlap at the detector. The third is the frame overlap chopper placed to prevent cross talk between frames. Fig. 1 shows a Daemen diagram, which illustrates how each of the choppers samples the moderator output, $\Lambda(t,\lambda)$.

The neutron wavelengths that reach the detector are the intersection of the areas defined between each pair of lines given by $\lambda = h/m(t_c-t)/L_c$,and $t - (mL_c/h)\lambda = t_c + \Delta t_c$, where L_c is the distance from the source to the chopper, t is the time that a neutron of wavelength, λ, is emitted from the moderator, and t_c, Δt_c are the time at which the chopper opens and the open duration, respectively. A simple diagram of the TOF versus distance from the source (Fig. 2) illustrates the opening and closing times for the three choppers needed on a 60 Hz, 1 ms (0.06 duty factor) LPSS SANS instruments.

The T_0 chopper limits the available band width at the detector. From a simple geometric argument, the wavelength bandwidth of neutrons emitted at the same time from the moderator passed by the chopper , $\Delta\lambda$, is related to the time interval over which the chopper is open by $\Delta\lambda = h/m(\Delta t_c /L_c)$. Thus, the best possible position for the T_0 chopper on a broad band instrument such as SANS is close to the source (minimize L_c) up to the limit that the maximum usable wavelength, $\lambda_{max} = {}^{h}/_{m}(n+p)\Delta T / L$, is passed. Here, n is the frame number after the pulse in which the neutron is counted and p is the number of source frequency intervals of duration, ΔT, between pulses used in the counting frame. These considerations give the optimal position as $L_c = (1-\Delta t_s / \Delta T)L/(n+p)$, where Δt is the source pulse length. Because the T_0 chopper is fixed in position, the upper and lower wavelengths that are likely to be used should be considered carefully and the T_0 chopper position determined accordingly, consistent with minimizing the maintenance and engineering difficulties of running a chopper in a high radiation environment. For a general purpose instrument, $\Delta\lambda$ is set by the lowest Q required and the dynamic range, and we take the former to be more important. We set Q_{min} to 0.002 $Å^{-1}$, and this requirement relates λ_{max} and L, through Eq. (1) in the subsequent optimization. The T_0 chopper position should be less than 5 m for a 60 Hz source, given the optimal instrument length determined below.

The frame definition and frame overlap chopper positions also affect $\Delta\lambda$. The spectrum passed by a chopper is given by the condition that the part of the spectrum, $\Lambda(t,\lambda)$, emitted at t by the source, is $t + (m/h)L_c$ such that λ falls within the interval over which the chopper is open. The range of wavelengths that is passed by the chopper is constant for the entire pulse width starting at $\lambda_{min} = {}^{h}/_{m}\left({}^{t_c}/_{L_c}\right)$, and has a bandwidth

$$\Delta\lambda = \frac{h}{m}\frac{\left(\Delta t_c - \Delta t_s\right)}{L_c}, \qquad 2$$

provided that $\Delta t_s < \Delta t_c$, which is a requirement for the existence of this region. This bandwidth defines the "umbra" shown in black in Fig. 2. There are two "penumbra" regions, shown in gray in Fig. 2, where the wavelengths sampled change linearly with TOF. The first "penumba" at small TOF starts at $\lambda'_{min} = {}^{h}/_{m}{}^{\left(t_c - \Delta t_s\right)}/_{L_c}$. At larger TOF there is a second "penumbra" starting at $\lambda''_{min} = {}^{h}/_{m}{}^{\left(t_c + \Delta t_c - \Delta t_s\right)}/_{L_c}$. The bandwidth of each penumbra region is $\Delta\lambda' = {}^{h}/_{m}\left({}^{\Delta t_s}/_{L_c}\right)$. This expression combined with the requirement that the full $\Delta\lambda$ fit within ΔT gives the relation,

$$\Delta T = \frac{L}{L_c}\left(\Delta t_c + \Delta t_s\right) - \Delta t_s. \qquad 3$$

Eq. (2) shows that the bandwidth of the "umbra" scales with Δt_c, and Eq. (2) and (3) taken together show that by moving the chopper away from the source as far as possible, Δt_c can be made as large as practical, thus increasing the fraction of the "umbra" in the TOF frame, as

$$\frac{\Delta t_u}{\Delta T} = \frac{L\left(\Delta t_c - \Delta t_s\right) + L_c \Delta t_s}{L\left(\Delta t_c + \Delta t_s\right) - L_c \Delta t_s}, \qquad 4$$

where Δt_u is the duration of TOF for the "umbra".

We used the LANSCE Monte Carlo instrument simulation code [4] to calculate the integral for the part of $\Lambda(t,\lambda)$ passed by the chopper system, taking into account the complete characteristics of $\Lambda(t,\lambda)$ computed for a coupled cold moderator and anticipated error in chopper phasing and jitter. From this calculation (Fig. 3) we see that the "penumbra effect" has a significant effect when the choppers are too close to the source on both λ_{min} and on the detector count rate (the area under each of the curves). We also use these calculations to determine the optimal disk chopper positions

from the source for a 60 Hz, 1 ms LPSS SANS to be between 4.2 and 5.6 m for the overlap chopper and greater than 7 m for the frame definition chopper.

SOURCE CHARACTERISTICS

The TOF resolution for SANS instruments at pulsed sources is affected by pulse width and shape. The count rate is determined by the total usable neutrons. Thus there is a balance between these two factors that must be considered in determining the optimal source characteristics. The SANS instrument is affected mostly by two characteristics: the peak brilliance and the peak shape. The latter is modeled by a main peak function convoluted with one or two exponential functions describing the tails of the pulse in time [5]. In SANS, the integrated $\Lambda(t,\lambda)$ contribute to the detector count rate is affected by both the peak height and width and the length of the exponential tail(s) parameterized by the time constant(s), τ. The peak width and the τ(s) contribute to the TOF resolution. The exponential tail length in a coupled moderator is determined by the material and geometry of the moderator/reflector system. Here, we assume a split-target/flux-trap moderator coupled to a composite Be-Pb reflector [1]. The values of τ varies with the thickness of the Be shell from 270 to 1700 μs (Fig. 4). We use the Monte Carlo instrument simulation package to integrate the different $\Lambda(t,\lambda)$ to obtain the TOF signal at the detector (Fig. 4). We note two effects: First, the value of λ at which the spectrum peaks, as measured at the detector, varies directly with τ. Second, the value of the integral over time, which is the total count at the detector, has a maximum for τ between 500 and 800 μs, assuming that all the neutrons passed by the chopper system are useful. For this range of τ, $\sigma(t) \approx \tau$ for the pulse. The condition for τ being consistent with the Q-resolution is,

$$\tau \leq \frac{1}{\sqrt{2}\,\hbar/m} L\lambda \frac{\sigma(Q)}{Q} = \frac{1}{\hbar/m} L\lambda \frac{\sigma(\theta)}{\theta'}, \text{ or } \frac{\lambda}{\theta'} \geq \frac{h}{m} \frac{\tau}{L\sigma(\theta)} \qquad 5$$

Thus, by choosing a particular moderator-reflector combination, and hence setting τ, we limit the usable ratio $\frac{\lambda}{\theta'}$ at a given L and angular resolution, $\sigma(\theta)$. The later two quantities are fixed for any given instrument configuration, and θ' is the minimum angle on the detector that data can be used consistent with $\sigma(Q)/Q$. Thus, the source characteristics of total neutron pulse length, given by τ, along with, $\sigma(\theta)$ and L determine the minimum wavelength and the fraction of the detector that can be used. This condition along with the frame overlap condition, gives the total band width as,

$$\max\left[\begin{array}{l}\dfrac{h}{m}\dfrac{\tau\theta'}{L\sigma(\theta)}, \text{resolution condition} \\ \dfrac{h}{m}\dfrac{n\Delta T}{L}, \text{frame overlap condition}\end{array}\right] \le \lambda \le \frac{h}{m}\frac{(n+p)\Delta T}{L}. \qquad 6$$

Thus, the choice of τ impacts the minimum wavelength that we can use for a given maximum value of $\sigma(\theta)/\theta$, but only if we chose to count in the first frame. The minimum wavelength is a linear function of τ, so that $\lambda_{min} \approx 1.7$ Å for $\tau = 750$ μs.

OPTIMIZATION

The optimal instrument configuration specified by the sample and detector positions requires that we maximize a figure of merit (FOM). We chose our FOM as

$$FOM = \frac{I(Q)}{\sigma^2(Q)} \ln\left(\frac{Q_{max}}{Q_{min}}\right). \qquad 7$$

The natural logarithm of the ratio of the maximum and minimum Q-values is the number of resolution elements in the reduced data, as $\sigma(Q)/Q \approx$ constant. Thus, this particular FOM corresponds with that derived from Shannon information theory [6].

Optimization was done by Monte Carlo simulation of a δ-scatterer , which scatters only at one Q value, and finding the instrument configuration with the maximum I(Q) at a given $\sigma(Q)$ and Q_{min}. Here, $\sigma(Q)/Q$ was set equal to 0.1, and Q_{min} was set at 0.002 Å^{-1}. We found that the optimal instrument length is different in the two cases studied, Q = 0.01and Q = 0.07 Å^{-1} (Fig. 5). The instrument length was 16 m for optimization at Q = 0.07 Å^{-1} and 18 m for optimization at Q = 0.01 Å^{-1}. In both cases, the sample position is at one half the source to detector distance (Fig. 5), which is in agreement with the cone rule.

Optimization for the Q = 0.07 Å^{-1} case is more sensitive to total instrument length than optimization for Q = 0.01 Å^{-1}. We can see why this is so from the R-T (detector radius versus TOF) in Fig. 6. Even with a large, 1 m detector, scattering at large Q runs off the detector if the instrument is too long. On the other hand if the sample to detector distance is too short, then the required Q-resolution cannot be achieved over the entire detector. This is because TOF channels differ in data quality at a given Q largely because the signal is taken from a different part of the detector [7,8]. Therefore, optimization of a SANS instrument using TOF is a balance of detector geometry needed to access a particular range of Q values and the Q-resolution needed for a particular measurement.

Because there are different optimal instrument lengths depending on the region of interest in Q, we conclude that TOF instrument built on a 60 Hz, 1MW LPSS should have a variable L, rather than a fixed length prevalent in first generation TOF instruments built on lower rep rate SPSS-type sources. This implies that the frame definition and frame overlap choppers be phased relative to the source to adjust the bandwidth of the instrument to match the length. This also implies that a variable entrance aperture size can be used to preserve the cone rule for focusing onto the detector.

COMPARISON OF INSTRUMENT PERFORMANCE FOR AN LPSS, SPSS AND CW (D11)

In our comparisons between continuous wave (CW), SPSS and LPSS instruments, each instrument is optimized for its particular type of source, using the methods described above, with $\sigma(Q)/Q$ equal to 10% at $Q = 0.01$ Å^{-1}. The CW source is the liquid hydrogen cold source CS-2 at the ILL. For the pulsed source instruments the output of a coupled, cold hydrogen moderator fed by a tungsten target is used. The proton pulse width is 1 μs and 1 ms, respectively for the SPSS and LPSS cases. For the LPSS a Be-Pb reflector is used. This gives a pulse with an exponential tail with $\tau = 734$ μs. A more weakly coupled Ni reflector is used for the SPSS with $\tau = 276$ μs. The SPSS gives about 10% less intensity than it would have had, had we simulated it for the more strongly coupled reflector used in the LPSS simulations [1]. However, the choice of a weaker coupled reflector for an SPSS is probably more realistic due to the need to service other, higher resolution instruments with the same facility. The SPSS source is simulated at 30 Hz, resulting is a duty factor ($3\ 10^{-5}$) that is closer to the optimal value for SANS. Intensity is calculated for the spallation sources given 1 MW total power. The CW source in calculated for a nominal 60 MW reactor, which is the power of the ILL HFR. The CW instrument uses a "monochromatic" incident neutron beam, which has a triangular probability distribution for λ with a 12% FWHM (9.8% $\sigma(\lambda)/\lambda$) spread. In the pulsed source instruments the neutron pulse is tailored by two choppers for an LPSS, and one chopper for an SPSS; both the LPSS and SPSS instruments have a T_0 chopper.

Comparisons among instruments on different sources depend on the measurement. Thus, we show two examples for optimized instruments at an LPSS, SPSS and CW. First, we look at the intensity and resolution of the instrument for a δ-scatterer at $Q = 0.01$ Å^{-1} (Table I). The LPSS case is not capable of obtaining a $Q_{min} = 0.002$ Å^{-1} with 10% resolution simultaneously. Either the resolution is better than the SPSS and CW cases or a different λ_{max} can be used resulting in a $Q_{min} = 0.0024$ Å^{-1} with a 10% resolution. For measurements at a single value of Q both the SPSS and

LPSS instruments perform comparable to D11 rescaled to the cold source CS-2 at the ILL (Table I).

We can extend the calculation to δ-scatterers for other Q values for the optimized instruments and for other instrument configurations, taking into account the variable detector position in our design, to calculate the response of each instrument as a function of Q. In Fig. 7 we compare the Q-resolution of the three instruments. An 18 m LPSS or SPSS has resolution comparable to D11 with a 21m configuration (Fig.7), and the 13 m pulse machines are close to the 10 m CW configuration. The count rates for 1 MW LPSS and SPSS and D11 rescaled to CS2 at 60 MW using different configurations are shown in Fig. 8. The 1 MW, 13 and 18 m pulsed instruments have count rates that are on the same order of magnitude with andabout half D11 rescaled for CS2 at comparable resolutions and Q range.

The response functions shown in Figs. 7 and 8 and in Table I do not give the entire picture. Details on the comparisons between different types of instruments depend on the requirements of the experiment. To illustrate this we looked at scattering from a spherical particle to simulate an actual measurement, asking the question: How much time is required to do a measurement over a given Q domain for a 'hard sphere' scatterer with R = 150 Å? The results are shown in Table II. The scattering measurements on a 30 Hz, 1MW SPSS require one configuration. The 60 Hz, 1MW LPSS requires two camera settings to obtain this same information, and takes approximately twice the measurement time. In the CW case, two or more camera settings would be required to cover the full Q range; however, the resolution for the higher Q range settings are very difficult to match to the pulsed source cases (see Fig. 7). The lowest camera setting for the CW case is tabulated in Table II and requires ~ 55 % longer measurement time relative to the 1MW SPSS case. If one is only interested in measuring a Guinier radius, then the 1MW LPSS measurement time is only ~ 35 % longer than the 1MW SPSS measurement time. Thus, even with the constraints of an LPSS at Los Alamos to be at 60 Hz, which limits the bandwidth or total length of a SANS instrument, the resulting machine will perform at a level comparable with the most intense instruments available today.

REFERENCES

1. E.J. Pitcher, G. J. Russell, P.A. Seeger, and P.D. Fergusson,, "Performance of Long-Pulse Source Reference Target-Moderator-Reflector Configurations", Proceedings of ICANS-XIII, Paul Scherrer Institut, Villigen, Switzerland, Oct. 11-14, 1995, pp. 323-329.
2. Proceedings of the Workshop on Neutron Instrumentation for a Long-Pulse Spallation Source, E. O. Lawrence Berkeley National Laboratory Report No. LBL-37880, Berkeley, California, April 18 - 21, 1995, pp II-23 - II-28.

3. W. Schmatz, T. Springer, J. Schelten, and K. Ibel, Neutron Small-Angle Scattering: Experimental Techniques and Applications , J. Appl. Cryst. 7, 96-116, 1974.
4. P. A. Seeger, "The MCLIB Library: Monte Carlo Simulation of Neutron Scattering Instruments", Proceedings of ICANS-XIII, Paul Scherrer Institut, Villigen, Switzerland, Oct. 11-14, 1995, pp. 194-212.
5. I. Ikeda and J. Carpenter, Wide-Energy-Range, High-Resolution Measurements of Neutron Pulse Shapes of Polyethlene Moderators, Nucl. Instr. Meth. **A239**, 536-544, 1985.
6. M. W. Johnson, The Information Bandwidth of Neutron Scattering Instruments, The Council for the Central Laboratory of the Research Councils, Rutherford Appleton Laboratory, Chilton, UK, Technical Report No. RAL-TR-95-011, 1995.
7. R.P. Hjelm, "Resolution of Time-of-Flight Low-Q diffractometers: Instrumental, Data Acquisition and Reduction Factors", *J. Appl. Crystal.*, **21**, 618-628 (1988).
8. P. A. Seeger and R. P. Hjelm, "Small-Angle Neutron Scattering at Pulsed Spallation Sources", *J. Appl. Crystal.*, **24**, 467-478 (1991).

Table 1

Scattering at Q = 0.01 $Å^{-1}$ for Optimized Configurations of LPSS, SPSS and CW

Source [a]	I(Q) (s^{-1}) [b]	σ(Q) ($Å^{-1}$) [c]	Q range ($Å^{-1}$) [d]
LPSS (λ_{max} = 10.7 Å; 18 m)	0.9 x 10^5	0.0008	0.002 - 0.048
LPSS (λ_{max} = 8.8 Å; 18 m)	2.1 x 10^5	0.001	0.0024 - 0.062
SPSS (λ_{max} = 10.7 Å; 18 m)	1.6 x 10^5	0.001	0.002 - 0.10
D11 @ ILL (10 Å, 21 m) using CS-2 cold source and CONSTANZE Velocity Selector	4.5 x 10^5	0.001	0.002 - 0.03

[a] Numbers in parentheses for LPSS and SPSS refer to the source to sample distance. The numbers for D11 refer to the mean wavelength and source to detector distance.

[b] The intensity values are for 1 MW for the LPSS and SPSS cases and 60 MW for D11.

[c] The rms of Q at Q = 0.01 $Å^{-1}$.

[d] The Q range accessed in a single instrument configuration, as noted.

Table II

Hard Sphere Scattering (R = 150 Å) for LPSS and SPSS

Source	Q-Range ($Å^{-1}$)	Time (s)	R (Å)	Rg (Å)
1MW SPSS (1 ms, 276 ms)	0.002 - 0.11	3.02	149.9 ± 0.9	115.8 ± 0.8
1MW LPSS (1 ms, 734 ms)	0.002 - 0.07 0.0035 - 0.13	4.08 2.01	148.6 ± 0.7	116.1 ± 0.6
D11@ILL (10 Å, 21m) using CS2 cold source and CONSTANZE velocity selector	0.002 - 0.029	1.7	141.3 ± 2.5	116.0 ± 0.6

Fig. 1: A Daemen diagram illustrating chopper sampling of moderator spectrum. Lines show the wavelength, λ, and time of emission, t, as viewed at the detector. Pairs of lines show the area sampled by each chopper: _____, T_0 chopper; — — —, frame definition chopper; - - - -, frame overlap chopper. The T_0 chopper blocks the initial pulse at $t \leq 0$ (wide line). The TOF to the detector is $t + (mL/h)\lambda$; thus, the detector sees a band of neutron wavelengths at each TOF interval that gives the TOF resolution of the experiment.

Fig. 2: The effect of T_o, frame definition and frame overlap chopper positions. The penumbra effect is shown. The closer the choppers are to the source, the greater the penumbra effect (light areas) and thus the smaller the useable flux in the frame.

Fig. 3: Effect of frame definition and frame overlap chopper positions on bandwidth. ●, T_0 chopper at 4 m, frame overlap chopper at 5.6 m, and frame definition chopper at 8.45 m; ■, T_0 chopper at 2.8 m, frame overlap chopper at 3.6 m, and frame definition chopper at 5.4 m.

Fig. 4: Effect of pulse tail on bandwidth at detector. ●, 1710 μs; ■, 1000 μs; ▵, 610 μs; ▿, 270 μs.

Fig. 5: Optimization of sample and detector positions for different Q-values. Upper frame, source to sample length, L_s,; lower frame, source to detector length, L. ●, $Q = 0.01$ Å^{-1}; ○, $Q = 0.07$ Å^{-1}.

Fig. 6: R-T plots of δ-scatterers. Vertical scale is TOF and horizontal is detector radius. Lines of intensity are at $Q = 0.01$ Å^{-1} and 0.07 Å^{-1}, as labeled. Upper panel is the simulation for a 16 m SANS on a 60 Hz, 1 ms LPSS. The lower panel is for an 18 m instrument.

Fig. 7: Resolution of LPSS, SPSS and CW instruments. Closed light boxes are for D11 at different instrument configurations with the shortest (3.6 m), to the longest (76 m), total length from top to bottom. The dark box is for the 18 m configuration of an LPSS. The actual resolution for an LPSS or CW instruments, are lines within each box parallel to the box bottom or top with σ inversely proportional to λ. The solid line is for an 18 m SPSS instrument, and the dished line is for a 13 m LPSS for $\lambda_{max} = 9.4$ Å.

Fig. 8: Count rates ad LPSS, SPSS and CW instruments. D11: __ __ __, 3.6 m λ= 4.5 Å; _ _ _ _,11 m λ=5.5 Å; __ _ __ _, 21 m λ= 10 Å. 18 m SPSS: __ _ _ __. LPSS: _____, 13 m λ_{max}=9 Å; hatched box 18 m and variable λ. The intensity increases with decreasing λ.

Fig. 1

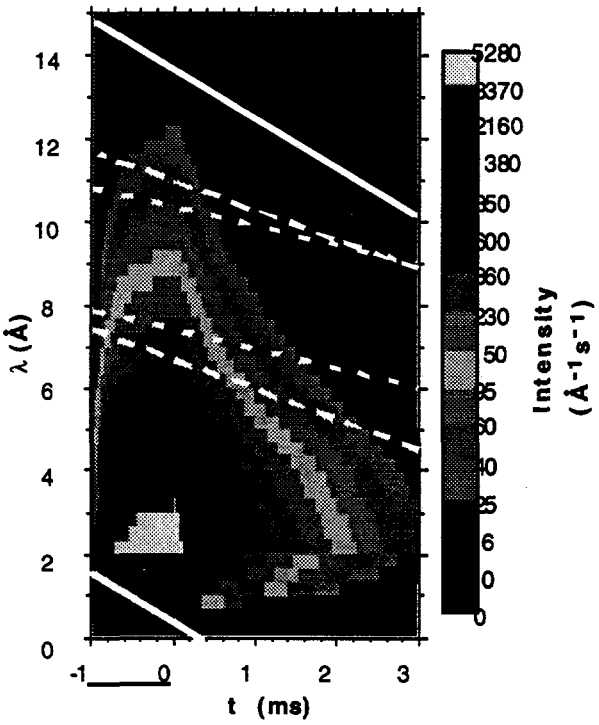
λ (Å)
t (ms)
Intensity
(Å⁻¹s⁻¹)
5280
3370
2160
380
650
500
360
230
50
25
10
40
25
6
0
0

Fig. 2

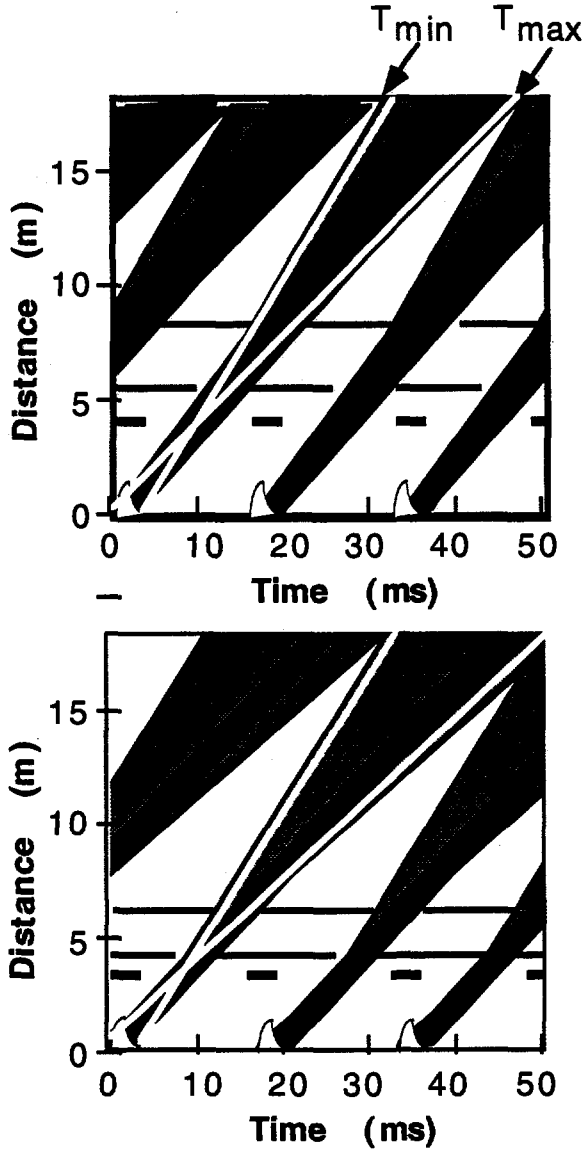
T min
T max
Distance (m)
15
10
5
0
0
10
20
30
40
50
Time (ms)
Distance (m)
15
10
5
0
0
10
20
30
40
50
Time (ms)

Fig. 3

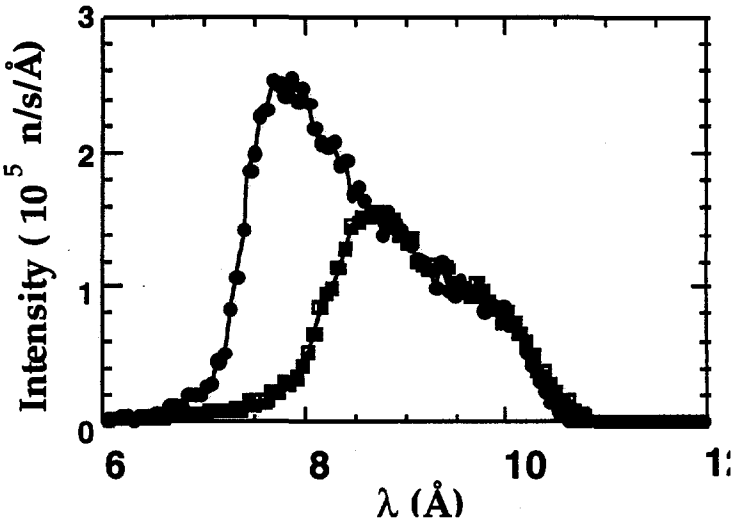

Fig. 4

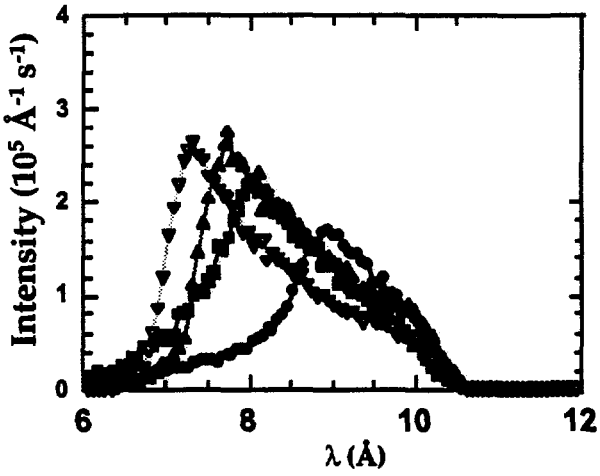

Fig. 5

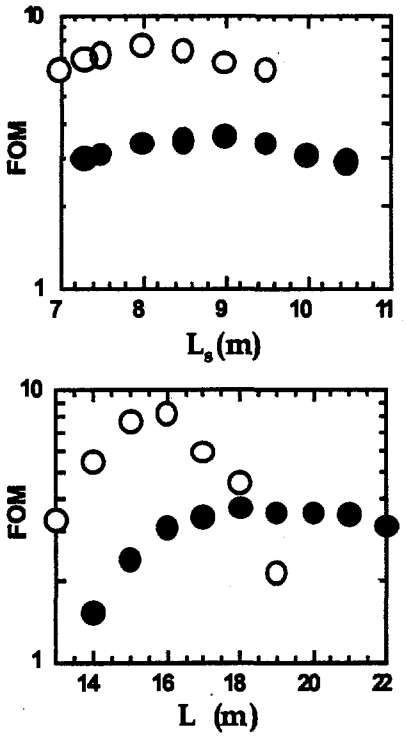

Fig. 6

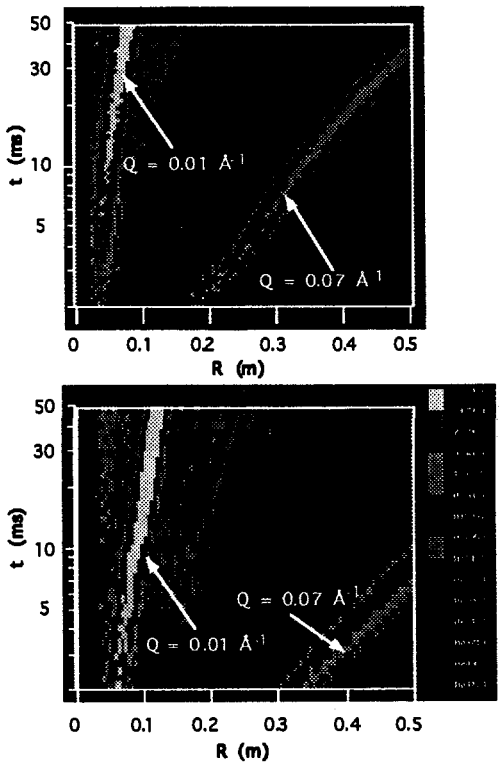
50
30
10
5
t (ms)
Q = 0.01 Å⁻¹
Q = 0.07 Å⁻¹
0
0.1
0.2
0.3
0.4
0.5
R (m)
50
30
10
5
t (ms)
Q = 0.07 Å⁻¹
Q = 0.01 Å⁻¹
0
0.1
0.2
0.3
0.4
0.5
R (m)

Fig. 7

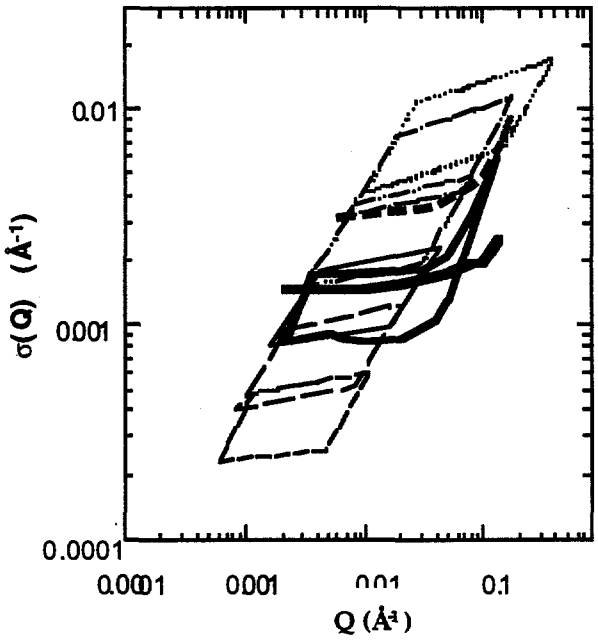

Fig. 8